Efficient and Accurate Computational Model of Neuron with Spike Frequency Adaptation

Zubayer Ibne Ferdous, Anlan Yu, Yuan Zeng, Xiaochen Guo, *Senior Member, IEEE*, Zhiyuan Yan, *Senior Member, IEEE*, and Yevgeny Berdichevsky, *Senior Member, IEEE*

***Abstract*— Simplified models of neurons are widely used in computational investigations of large networks. One of the most important performance metrics of simplified models is their accuracy in reproducing action potential (spike) timing. In this article, we developed a simple, computationally efficient neuron model by modifying the adaptive exponential integrate and fire (AdEx) model** [1] **with sigmoid afterhyperpolarization current (Sigmoid AHP). Our model can precisely match the spike times and spike frequency adaptation of cortical pyramidal neurons. The accuracy was similar to a more complex two compartment biophysically realistic model of the same neurons. This work provides a simplified neuronal model with improved spike timing accuracy for use in modeling of large neural networks.**

***Clinical Relevance*— Accurate and computationally efficient single neuron model will enable large network modeling of brain regions involved in neurological and psychiatric disorders and may lead to a better understanding of the disorder mechanisms.**

I. Introduction

Development of neuron models to explain neuronal dynamics has a long history. Biophysically accurate models such as the *Traub* model [2] and the *Pinsky-Rinzel* model [3] were based on Hodgkin-Huxley model and explained membrane potential dynamics of a hippocampal neuron using numerous gated ion channels. In this framework, multiple differential equations are required to model a single gated ion channel, and due to fast dynamics of sodium and potassium voltage gated channels, small time steps are required for simulation stability. These disadvantages make modeling of large networks with biophysically accurate neuronal models prohibitively computationally expensive. At the other end of the complexity spectrum is the simple integrate-and-fire (IF) model which models action potentials with a threshold function. IF model is able to produce spikes in response to stimulation, but spike timing is determined only by membrane resistance, capacitance, and the magnitude of the injected current, and is not accurate. Other models such as *Exponential Integrate and Fire* [4] and *Quadratic Integrate and Fire* model [5] incorporated more complex action potential generation into the base IF model but lacked spike frequency adaptation found in pyramidal neurons of the cortex. Adaptation was incorporated into *Izhikevich* [6] and the AdEx [7] models which could replicate general firing patterns of fast spiking interneurons and thalamo-cortical neurons. However, these models were not shown to accurately match timing of spikes evoked by a wide range of current inputs, particularly in cortical pyramidal cells. In the AdEx model, the membrane voltage has an exponential upswing at the threshold to spike followed by a numerical reset after each spike. Additionally, each spike increases the after hyperpolarization (AHP) current by a constant amount to explain spike-triggered adaptation *(described in methods)*. In this work, we replaced the activation of the AHP current in the existing AdEx model by a sigmoid function to match timing of spikes evoked by varying levels of current injection.

Precise spike timing is of paramount importance to studies of spike time dependent synaptic plasticity [8], formation of memory engrams [9], understanding of spatiotemporal memory processes [10], among many others. *Fitz et al. 2020* [11] showed that semantic information may be stored in the AHP variable of a neuron for sequential language processing. Thus, development of a simplified neuronal model that can accurately predict spike timing based on current input may contribute to computational studies of brain networks and their disorders.

In this work, we recorded the membrane potential of cortical excitatory neurons after different levels of current injection (25 pA to 275 pA with a Δstep of 25 pA) at a frequency of 5 Hz, which is in the range of activating long term plasticity. We then determined whether our new Sigmoid AHP model can match experimentally obtained spike times better than the established AdEx model. We also compared the performance of the Sigmoid AHP model to the biophysically accurate Pinsky-Rinzel model in matching the spike timing.

II. Method

A. Culture preparation and Experimental procedure

Cultures of dissociated cortical neurons were prepared from post-natal day 0–1 Sprague-Dawley rat pups (Charles River Laboratories) as described earlier [12]. On day in vitro (DIV) 11 to 20, we replaced the culture medium with an artificial cerebrospinal fluid (ACSF) solution (at 37ºC) for performing whole cell current clamp recordings. The ACSF solution contained (in mM): 140 NaCl, 2.4 KCl, 10 HEPES, 10 glucose, 2 $CaCl_2$, 1 $MgCl_2$, 1 Na_2HPO_4 (p H 7.4) [13]. Recording electrodes had 5-10 MΩ resistance when filled with internal solution containing (in mM): 130 k-gluconate, 10 HEPES, 10 phosphocreatine, 5 KCl, 1 $MgCl_2$, 4 ATP-Mg and 0.3 mM GTP [14]. Recordings were acquired at 10 kHz.

*Research was supported by NSF NCS-FO.

Zubayer Ibne Ferdous, Anlan Yu, Yuan Zeng, Xiaochen Guo, and Zhiyuan Yan are with the Electrical and Computer Engineering, Lehigh University, Bethlehem, PA 18015, USA (Z. I. Ferdous is the corresponding author, email: zui216@lehigh.edu)

Yevgeny Berdichevsky is with the Electrical and Computer Engineering and the Department of Bioengineering, Lehigh University, Bethlehem, PA 18015, USA

B. Pinsky-Rinzel Model

We adapted a two compartmental Pinsky-Rinzel model [3]. Briefly, the model consists of one soma and one dendritic compartment with ionic currents for each compartment, the coupling conductance between compartments, and Ca^{2+} concentration in the dendritic compartment. The soma compartment has one Na^{+} transient channel (I_{Na}) and one delayed rectifier K^{+} channel (I_{K-DR}). The dendritic compartment has one slow after hyperpolarization K^{+} channel (I_{K-AHP}), one rapid voltage and Ca^{2+} dependent K^{+} channel (I_{K-C}), and one high-threshold voltage dependent Ca^{2+} channel (I_{Ca}). Keeping the governing equations same as the existing model [3], we modified the maximum conductance of each ionic channel and its gating variables (activation and inactivation parameters) to fit the experimental results of our dissociated cortical neurons. All simulations were performed in NEURON at 0.025 ms time step. The neuron model [3] was obtained from *ModelDB (accession number 35358)*.

C. AdEx and Sigmoid AHP Model

The governing equations for AdEx model [1] are,

$$\tau_m \frac{du}{dt} = -(u - u_{rest}) + \Delta_T \exp\left(\frac{u - \vartheta_{rh}}{\Delta_T}\right) - Rw + RI$$

$$\tau_w \frac{dw}{dt} = -w + a(u - u_{rest}) + b\sum_{tf} \delta(t - t^f)$$

Here, u is the absolute membrane potential with resting potential of u_{rest} and w is the AHP current. τ_m and τ_w are the time constants. The AHP current is fed back to the voltage equation with resistance, R. The sharpness of the action potential is controlled by Δ_T and threshold voltage ϑ_{rh}. I is the input current injection. The voltage, u is reset if the membrane potential reaches the numerical threshold θ_{reset}. After firing, integration of the voltage restarts at $u = u_r$. a is the coupling of voltage to adaptation. t^f represents timing of spikes indicating each spike will increase the AHP current by a constant b. We modified the AdEx model by introducing a sigmoid function in the AHP variable to resemble the dynamic behavior of the intracellular Ca^{2+} gated K^{+} channel:

$$\tau_w \frac{dw}{dt} = -w + b\sum_{tf} \delta(t - t^f) * \left(p + \frac{q}{1+exp(-r(w-s))}\right)$$

In sigmoid AHP, each spike will increase the AHP current by b multiplied by a sigmoid function of the previous value of AHP. $p, q, r, and\ s$ are tunable parameters that determine how the change in adaptive current will be influenced by its previous level. All simulations were performed in MATLAB at 1 ms time step. Parameters of Sigmoid AHP and Pinsky-Rinzel model were optimized for neuron properties measured at 37ºC (Data shared at doi.org/10.6084/m9.figshare.14838402.v7).

D. Evaluation Metric

To evaluate the model fitting for 10 neurons, we measured the relative error of time to first and second spikes (T_{AP}^1 and T_{AP}^2, respectively) and adaptivity index ($A.Index$) for each current injection (25 pA to 275 pA with a Δstep of 25 pA). Adaptivity index was defined as the ratio of the final inter-spike interval (ISI) over the first inter-spike interval, ISI_{final}/ISI_{first}. Relative error of each metric for each injected current was expressed as $|exp - model|/exp$.

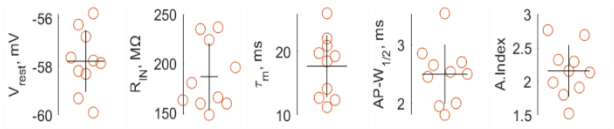

Figure 1: Selection of 10 excitatory neurons for model fitting. Resting potential (V_{rest}, mV), Input resistance (R_{IN}, MΩ), Time constant (τ_m, ms), Spike half-width ($AP - W_{1/2}$, ms), Adaptivity Index ($A.Index$) of 10 neurons (shown in red circles). Mean and standard deviation of 10 excitatory neurons are shown in black horizontal and vertical lines, respectively.

III. Results

We injected current at a frequency of 5 Hz with 100 ms pulse-width *(described in methods)* to 10 excitatory neurons and measured the membrane potential. Then we characterized several neuron properties (Resting potential (V_{rest}), input resistance (R_{IN}), time constant τ_m, half-width of spike $AP - W_{1/2}$, and adaptivity index ($A.Index$)) based on the current clamp data. Mean and standard deviation of these properties are shown in Fig. 1 (black horizontal and vertical lines, respectively). To evaluate our sigmoid AHP model, we fitted these 10 neurons using one set of parameters per neuron and quantified the error for each current injection and the overall relative error. We then compared these results with the results obtained via the biophysical Pinsky-Rinzel model.

Optimization of the parameters to best fit the experimental results was done in three steps for both AdEx and sigmoid AHP models. First, membrane time constant τ_m and input resistance R were determined by matching the potential response to the lowest negative input current (-25 pA). Second, time to first spike (T_{AP}^1) was only a function of the exponential term in the first model equation. So, the absolute difference between the experiment and model for the time of the first spike (relative to the beginning of current injection) was minimized by tuning Δ_T and ϑ_{rh}. Third, the two other evaluation metrics (time to second spike (T_{AP}^2) and adaptivity index) were controlled by the AHP current, w. Parameters related to w were iteratively tuned until the average relative errors to all current inputs of both time to second spike and adaptivity index were below 20%.

Although AdEx model was able to match T_{AP}^1, it could not provide a good fit for both T_{AP}^2 and adaptivity index (Fig. 2B top and middle panel) for each current input. Since the AdEx increases the AHP current by a constant amount after each spike, it could either fit the experimental T_{AP}^2 (Fig. 2B top panel when time constant of the AHP current, τ_w is small) or adaptivity index (Fig. 2B middle panel when τ_w is large). We hypothesized that the AHP current remains small after the first spike but increases rapidly after the subsequent spikes due to intracellular [Ca^{2+}] dynamics. To implement this idea, we used a sigmoid increase of AHP current in our model that could fit the experimental data for all current inputs (Fig. 2B bottom panel). As expected, the maximum amplitude of the AHP current (shown as yellow traces in all panels of Fig. 2B) with the AdEx was nearly uniform for small τ_w and slowly increasing for large τ_w, but it rapidly transitioned to a much larger value with the sigmoid AHP following high frequency firing. Average relative error for the neuron shown in Fig. 2B with all current inputs with the sigmoid AHP model was 4% for T_{AP}^1, 8% for T_{AP}^2 and 10% for adaptivity index. Whereas the

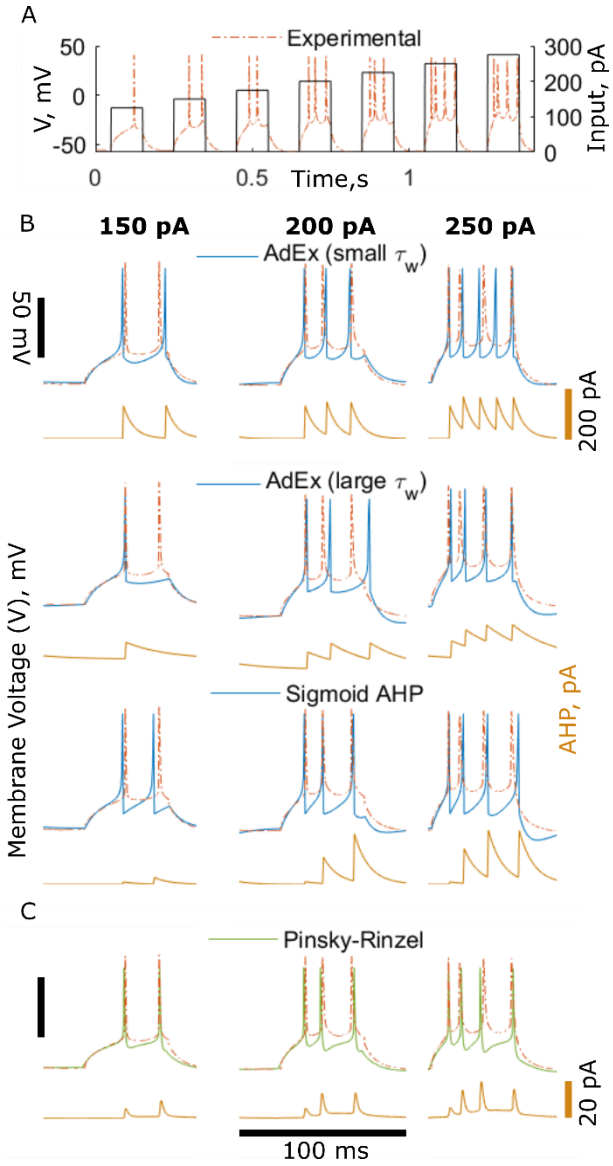

Figure 2: Model fitting of experimental I-V curves of one neuron. (A) Traces of injected current (black line, right y axis) and membrane potential (red dashed line, left y axis) from the experiment. (B) Simulation of the experimental fits for three current injections (left: 150 pA, middle: 200 pA, right: 250 pA). The AdEx model with large τ_w (blue line; top panel), The AdEx model with small τ_w (blue line; middle panel) and the sigmoid AHP model (blue line; bottom panel). Yellow line in all panels indicates the AHP variable (C) Fitting Pinsky-Rinzel model to the experimental trace for the same three current injections (left: 150 pA, middle: 200 pA, right: 250 pA) of the same neuron. Yellow line represents the AHP current ($I_{K-AHP} + I_{K-C}$) from the Pinsky-Rinzel. Vertical scalebar at left in panel (B & C) indicates 50 mV. Vertical scalebar at right indicates 200 pA in panel B and 20 pA in panel C. Both panel B & C have the same horizontal scalebar of 100 ms.

average relative error with the AdEx model (small τ_w), was for 4% T_{AP}^1, 11% for T_{AP}^2 and 45% for adaptivity index and the average relative error with the AdEx model (large τ_w), was for 10% T_{AP}^1, 25% for T_{AP}^2 and 22% for adaptivity index.

We then fit the experimental data using Pinsky-Rinzel model (Fig. 2C). Crosstalk of nearly 50 parameters in the Pinsky-Rinzel equations lead to an iterative approach to match the experimental data. Similar to the initial step applied with the previous models, we tuned the capacitance and leakage channel to fit the potential for the lowest negative current input Na channel and K-DR channel from the soma compartment; Ca channel, K-AHP channel and K-C channel from the dendrite compartment were determined by matching T_{AP}^1, T_{AP}^2 and adaptivity index with each positive current injection for each neuron. Maximum conductances and some non-trivial gating parameters were tuned for a tradeoff between complexity and modeling accuracy. Parameter combinations that achieved the smallest error metric were selected. The equivalent AHP current ($I_{K-AHP} + I_{K-C}$) from the Pinsky-Rinzel (yellow trace in Fig. 2C) had the similar dynamics as the AHP current from the sigmoid AHP (yellow trace in the bottom panel of Fig. 2B). AHP current of the Pinsky-Rinzel model have a different amplitude compared to AdEx and sigmoid AHP, because the former also had a K^+ rectifier current to repolarize the membrane voltage. Average relative error for the neuron shown in Fig. 2 with all current inputs for Pinsky-Rinzel was 3% for T_{AP}^1, 4% for T_{AP}^2 and 16% for adaptivity index. Both sigmoid AHP and Pinsky-Rinzel model yielded close match with the experimental findings of this neuron.

Next, we compared our evaluation metrics between 10 experimental neurons fitted by the sigmoid AHP and by the Pinsky-Rinzel model (Fig. 3). Relative errors of T_{AP}^1, T_{AP}^2, and adaptivity index were measured for each spike-evoking current input (Fig. 3A top, middle, and bottom panel respectively). No neuron had more than one spike with 100 pA current input and more than two spikes with less than 175 pA current input. Relative errors with any current input were not over 15% for T_{AP}^1, 10% for T_{AP}^2, and 20% for $A.index$ with sigmoid AHP (blue dots and blue boxplots in Fig. 3A). Similarly, they were not over 8% for T_{AP}^1, 10% for T_{AP}^2, and 30% for $A.index$ with Pinsky-Rinzel (green dots and green boxplots in Fig. 3A). Finally, we drew an overall comparison between the two models by taking the median of relative errors for all current inputs per neuron (Fig. 3B). The upper range (75th percentile) for [T_{AP}^1, T_{AP}^2, $A.index$] was [3%, 5%, 15%] with sigmoid AHP and [4%, 5%, 24%] with Pinsky-Rinzel model.

IV. Discussion

In this work, we developed a fast computational model of a single neuron that could generate realistic timing of neuronal spiking due to input current. Sigmoid AHP model achieved spike timing accuracy that was comparable to or better than biophysically accurate Pinsky-Rinzel model. High accuracy of the Sigmoid AHP model was achieved by implementing an AHP current with sigmoid dynamics that approximated Ca^{2+} gating: spike triggered AHP current had a rapid increase after the evocation of more than one spike. This idea agrees with *Andrade et al. 2012* [15] that demonstrated Ca^{2+} dependent afterpotential as a function of spike frequency. Because of the smaller number of equations and larger time steps compared to the Pinsky-Rinzel model, we expect that Sigmoid AHP model will be substantially less computationally expensive when used in large network simulations. Due to its accuracy in matching spike timing, this

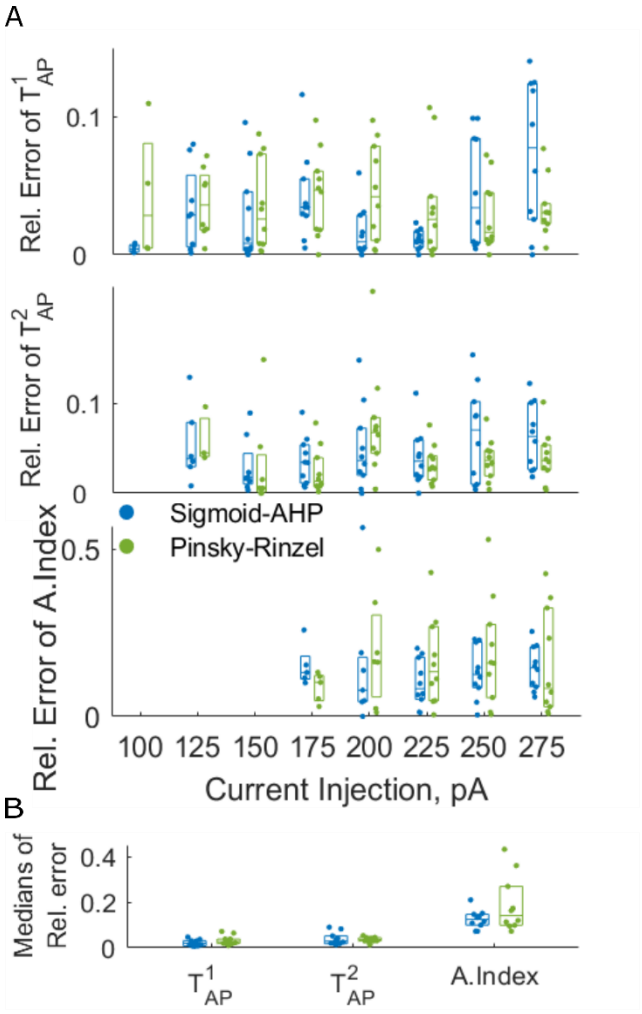

Figure 3: Evaluation of modeling results as relative error (Rel. error) and their comparison. (A) (Top panel) Relative error of time to 1st AP (T^1_{AP}) was measured for each current injection. Each dot (blue for sigmoid AHP and green for Pinsky-Rinzel model, respectively) indicates one neuron that evokes at least one spike during the input current pulse. Boxplot shows the median (middle line), 25th (bottom line), and 75th (top line) percentile of the relative error for different current injection. (Middle panel) Same as top panel, but for the relative error of time to 2nd AP (T^2_{AP}). (Bottom panel) Same as top panel, but for the relative error of adaptivity index ($A.Index$). (B) Each dot (blue for sigmoid AHP and green for Pinsky-Rinzel model, respectively) here represents the median of relative errors for all input current pulses for one neuron. Relative errors of each metric are shown in the x axis. Boxplot shows the median (middle line), 25th (bottom line), and 75th (top line) percentile of the data.

model can be used in spiking neural network studies of supervised learning algorithms [16] or drug application [17], among many others.

References

[1] W. Gerstner, W. M. Kistler, R. Naud, and L. Paninski, *Neuronal dynamics: From single neurons to networks and models of cognition*. 2014.

[2] R. D. Traub, R. K. S. Wong, R. Miles, and H. Michelson, "A model of a CA3 hippocampal pyramidal neuron incorporating voltage-clamp data on intrinsic conductances," *J. Neurophysiol.*, vol. 66, no. 2, pp. 635–650, 1991, doi: 10.1152/jn.1991.66.2.635.

[3] P. F. Pinsky and J. Rinzel's, "Intrinsic and network rhythmogenesis in a reduced traub model for CA3 neurons," *J. Comput. Neurosci.*, vol. 2, no. 3, p. 275, 1995, doi: 10.1007/BF00961439.

[4] N. Fourcaud-Trocmé, D. Hansel, C. Van Vreeswijk, and N. Brunel, "How Spike Generation Mechanisms Determine the Neuronal Response to Fluctuating Inputs," *J. Neurosci.*, vol. 23, no. 37, pp. 11628–11640, 2003, doi: 10.1523/jneurosci.23-37-11628.2003.

[5] P. E. Latham, B. J. Richmond, P. G. Nelson, and S. Nirenberg, "Intrinsic dynamics in neuronal networks. I. Theory," *J. Neurophysiol.*, vol. 83, no. 2, pp. 808–827, 2000, doi: 10.1152/jn.2000.83.2.808.

[6] E. M. Izhikevich, "Simple model of spiking neurons," *IEEE Trans. Neural Networks*, vol. 14, no. 6, pp. 1569–1572, 2003, doi: 10.1109/TNN.2003.820440.

[7] R. Brette and W. Gerstner, "Adaptive exponential integrate-and-fire model as an effective description of neuronal activity," *J. Neurophysiol.*, vol. 94, no. 5, pp. 3637–3642, 2005, doi: 10.1152/jn.00686.2005.

[8] A. Kumar and M. R. Mehta, "Frequency-dependent changes in NMDAR-dependent synaptic plasticity," *Front. Comput. Neurosci.*, vol. 5, no. September, pp. 1–15, 2011, doi: 10.3389/fncom.2011.00038.

[9] X. Zhang, F. C. Yeh, H. Ju, Y. Jiang, G. F. W. Quan, and A. M. J. Vandongen, "Familiarity detection and memory consolidation in cortical assemblies," *eNeuro*, vol. 7, no. 3, pp. 1–19, 2020, doi: 10.1523/ENEURO.0006-19.2020.

[10] H. Ju, M. R. Dranias, G. Banumurthy, and A. M. J. Vandongen, "Spatiotemporal memory is an intrinsic property of networks of dissociated cortical neurons," *J. Neurosci.*, vol. 35, no. 9, pp. 4040–4051, 2015, doi: 10.1523/JNEUROSCI.3793-14.2015.

[11] H. Fitz, M. Uhlmann, D. Van Den Broek, R. Duarte, P. Hagoort, and K. M. Petersson, "Neuronal spike-rate adaptation supports working memory in language processing," *Proc. Natl. Acad. Sci. U. S. A.*, vol. 117, no. 34, pp. 20881–20889, 2020, doi: 10.1073/pnas.2000222117.

[12] Y. Ming, M. F. Hasan, S. Tatic-Lucic, and Y. Berdichevsky, "Micro Three-Dimensional Neuronal Cultures Generate Developing Cortex-Like Activity Patterns," *Front. Neurosci.*, vol. 14, no. October, pp. 1–13, 2020, doi: 10.3389/fnins.2020.563905.

[13] H. Yamamoto, R. Matsumura, H. Takaoki, S. Katsurabayashi, A. Hirano-Iwata, and M. Niwano, "Unidirectional signal propagation in primary neurons micropatterned at a single-cell resolution," *Appl. Phys. Lett.*, vol. 109, no. 4, 2016, doi: 10.1063/1.4959836.

[14] J. Barral and A. D'Reyes, "Synaptic scaling rule preserves excitatory-inhibitory balance and salient neuronal network dynamics," *Nat. Neurosci.*, vol. 19, no. 12, pp. 1690–1696, 2016, doi: 10.1038/nn.4415.

[15] R. Andrade, R. C. Foehring, and A. V. Tzingounis, "The calcium-activated slow AHP: Cutting through the Gordian Knot," *Front. Cell. Neurosci.*, vol. 6, no. OCTOBER 2012, pp. 1–38, 2012, doi: 10.3389/fncel.2012.00047.

[16] J. Xin and M. J. Embrechts, "Supervised learning with spiking neural networks," *Proc. Int. Jt. Conf. Neural Networks*, vol. 3, no. 3, pp. 1772–1777, 2001, doi: 10.1109/ijcnn.2001.938430.

[17] B. L. Foster, I. Bojak, and D. T. J. Liley, "Population based models of cortical drug response: Insights from anaesthesia," *Cogn. Neurodyn.*, vol. 2, no. 4, pp. 283–296, 2008, doi: 10.1007/s11571-008-9063-z.